

The photoproduction of P_c in $\gamma p \rightarrow J/\psi p$ and the feed down phenomenon of P_c

段鸣晓(Ming-Xiao Duan)

合作者：邱林、赵强

Institute of High Energy Physics

August 13, 2024 to August 18, 2024

山东·青岛

第十四届全国粒子物理学术会议

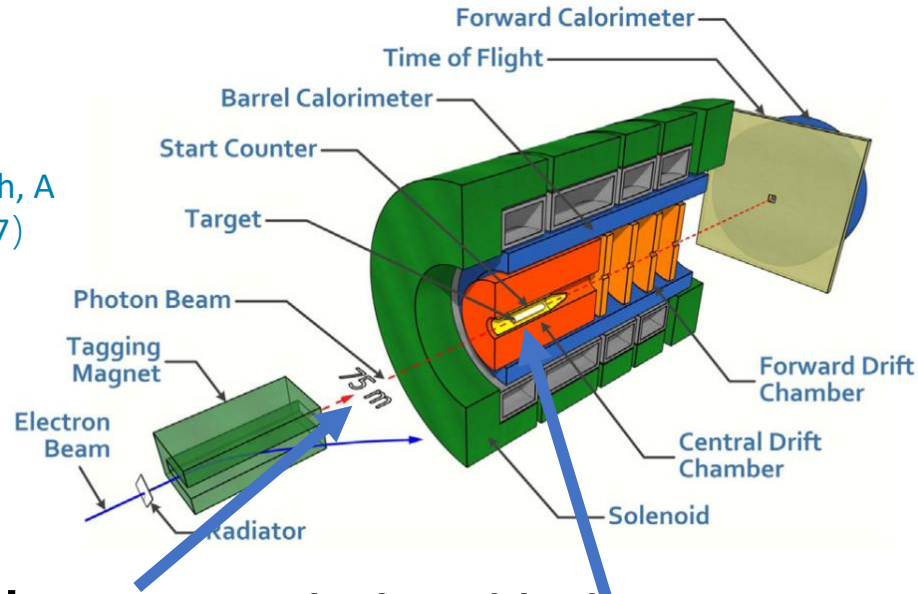
Content

- I. A brief Introduction of the J/ψ photoproduction from GluX.
- II. The photoproduction of the P_c in our formalism.
- III. Numerical results.
- IV. The feed down phenomenon of P_c .
- V. Summary.

Measurements on $\gamma p \rightarrow J/\psi p$

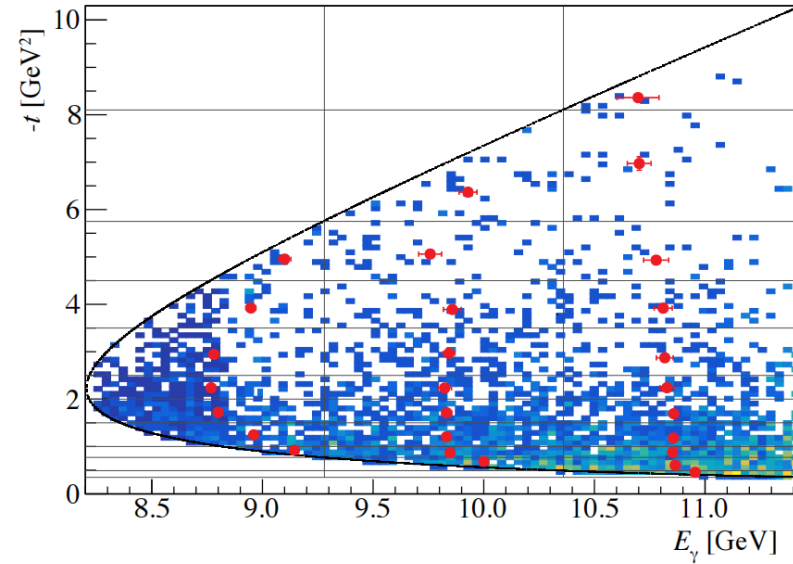
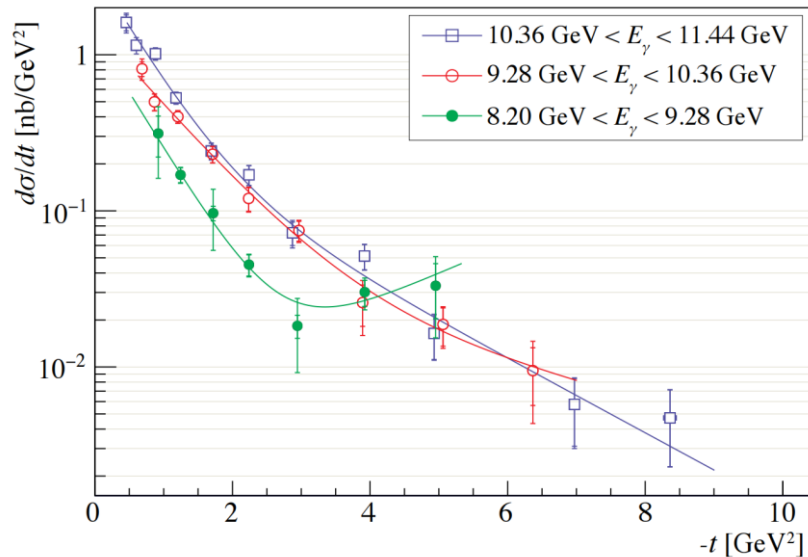
GlueX

(Physics Research, A
987 (2021) 164807)

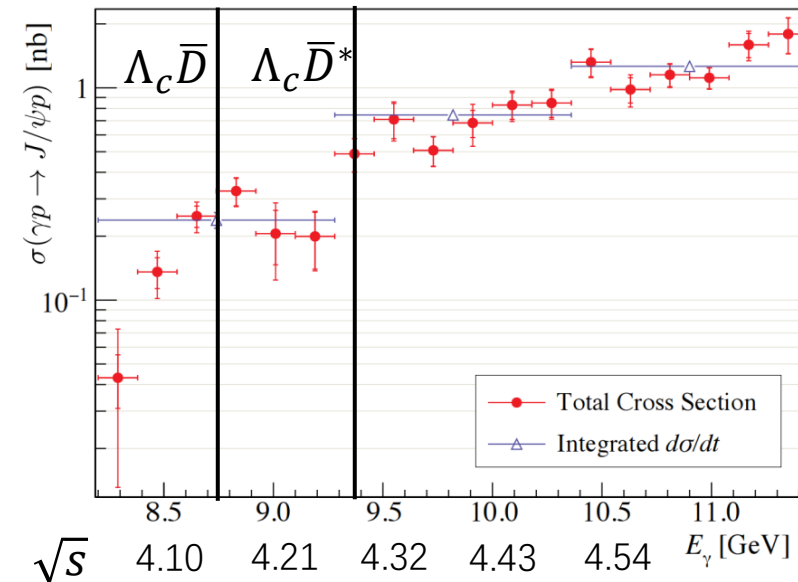


Real photon The liquid-hydrogen target

$d\sigma/dt$



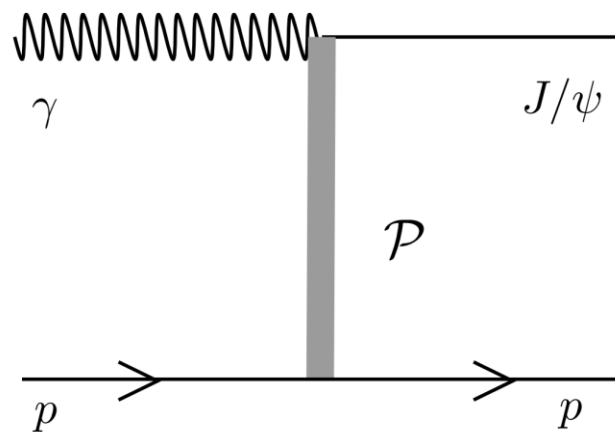
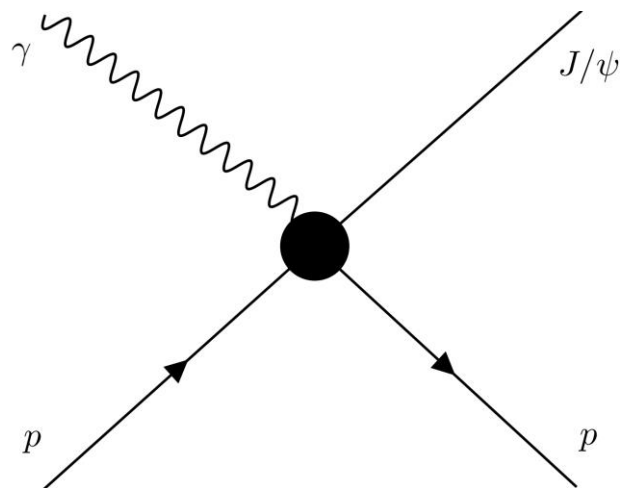
arXiv:2304.03845v1
Phys.Rev.C 108 (
2023) 2, 025201



$\sigma(s)$

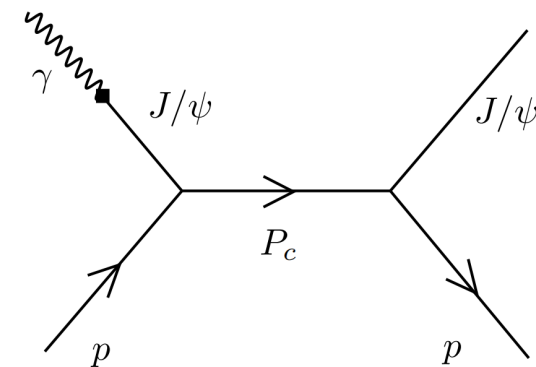
structures around
the $\Lambda_c \bar{D}$ threshold
appear in the cross
section data.

Analysis on $\gamma p \rightarrow J/\psi p$



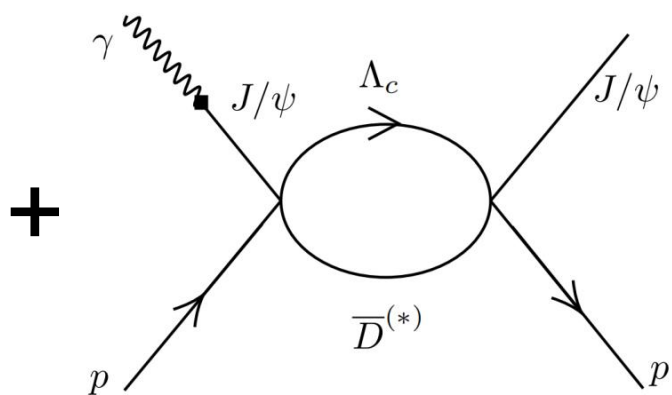
Pomeron exchange

+

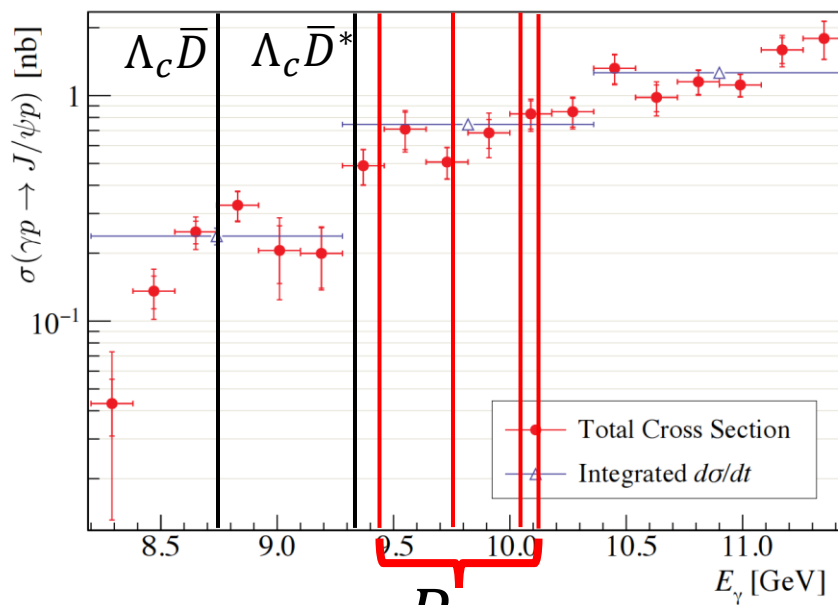


Pc intermediate states

Tree level

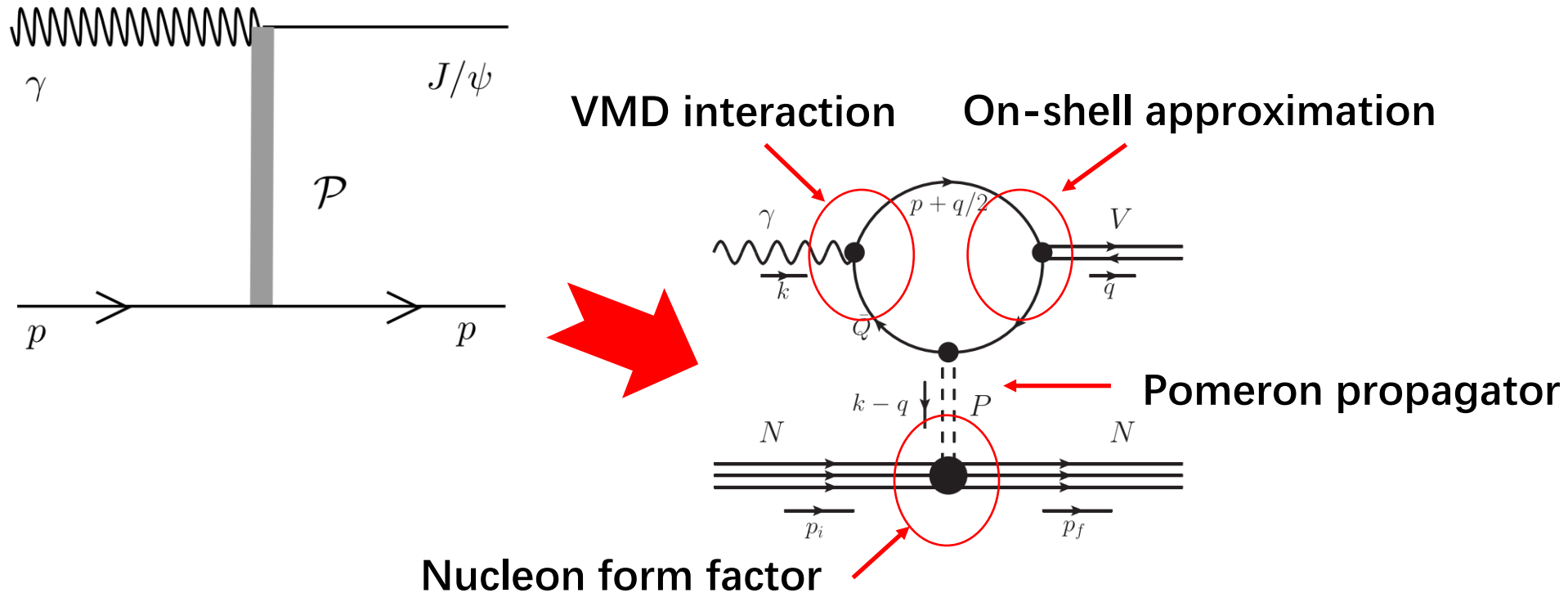


One Loop



Where are the Pc states ?

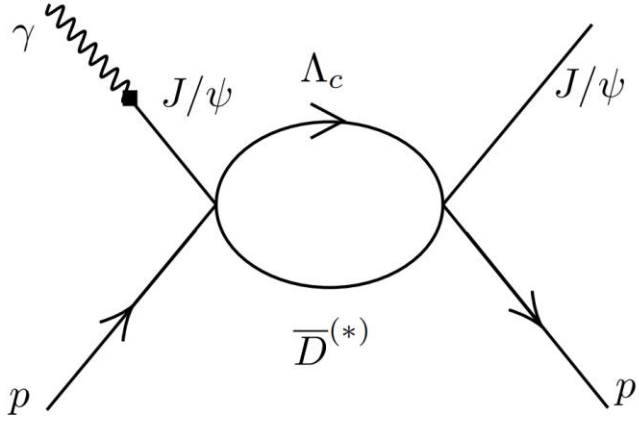
Analysis on $\gamma p \rightarrow J/\psi p$



$$\mathcal{M}^{\mathcal{P}} = \frac{eM_{J/\psi}^2}{f_{J/\psi}} \varepsilon_{\gamma\nu} \left[2\beta_c T^{\alpha,\mu\nu} \frac{4\mu_0}{(M_{J/\psi}^2 - t)(2\mu_0^2 + M_{J/\psi}^2 - t)} \right] \varepsilon_{J/\psi\mu}^* \\ \times \bar{u}(p') F_\alpha(t) u(p) \left[-i(\alpha' s)^{\alpha-1} \right].$$

$$T^{\alpha,\mu\nu} = (k + q)^\alpha g^{\mu\nu} - 2k^\nu g^{\alpha\mu} \\ F_\alpha(t) = 3\beta_0 \gamma_\alpha \frac{4M_p^2 - 2.8t}{(4M_p^2 - t)(1 - t/0.7)^2}$$

Analysis on $\gamma p \rightarrow J/\psi p$



$$\begin{aligned}
 & \int d^4q_1 e^{-\frac{2|\mathbf{q}_1|^2}{\Lambda^2}} / (q_1^2 - m_{q_1}^2 + i\varepsilon)(q_2^2 - m_{q_2}^2 + i\varepsilon) \\
 & \approx \frac{1}{4m_{q_1}m_{q_2}} \int d^4q_1 d^4q_2 \frac{e^{-\frac{2|\mathbf{q}_1|^2}{\Lambda^2}}}{(q_1^0 - m_{q_1} - \frac{|\mathbf{q}_1|^2}{2m_{q_1}} + i\varepsilon)(\sqrt{s} - q_1^0 - m_{q_2} - \frac{|\mathbf{q}_2|^2}{2m_{q_2}} + i\varepsilon)} \\
 & = \frac{2\pi i}{4m_{q_1}m_{q_2}} \int d^3\mathbf{q}_1 \frac{e^{-\frac{2|\mathbf{q}_1|^2}{\Lambda^2}}}{\sqrt{s} - m_{q_1} - m_{q_2} - \frac{|\mathbf{q}_1|^2}{2m_{q_1}} - \frac{|\mathbf{q}_2|^2}{2m_{q_2}}} \\
 & = \frac{i(2\pi)^3}{4m_{q_1}m_{q_2}} \left[\frac{\mu\Lambda}{\sqrt{2\pi}} + \mu k e^{-2k^2/\Lambda^2} (-erfi[\frac{\sqrt{2}k}{\Lambda}] + i) \right].
 \end{aligned}$$

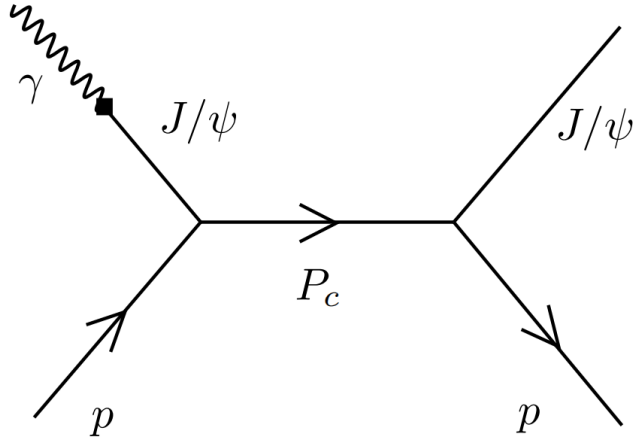
$$\mathcal{L}_{J/\psi p \Lambda_c \bar{D}^{(*)}} = ig_x \psi^\nu \bar{N} \gamma_5 \gamma_\mu \Lambda_c \bar{D} + g_{x^*} \bar{N} \Lambda_c \psi^\nu D_{\mu}^{*}$$

$$\mathcal{L}_{VMD} = -\frac{em_{J/\psi}^2}{f_{J/\psi}} V \cdot A$$

$$\begin{aligned}
 \mathcal{M}_{\Lambda_c \bar{D}} &= \int \frac{d^4q_1}{(2\pi)^4} ig_x^2 \frac{eM_{J/\psi}^2}{f_{J/\psi}} \bar{u}_p(p_4, m_4) \gamma_5 \gamma_\mu (\not{q}_1 + m_1) \\
 & \times \gamma_\nu \gamma_5 u_p(p_2, m_2) \varepsilon_{J/\psi}^{*\mu}(p_3, m_3) \varepsilon_{\gamma\alpha}(p_1, m_1) \\
 & \times \frac{g^{\nu\alpha} \mathcal{F}^2(q_1^2, \Lambda^2)}{(q_1^2 - m_{q_1}^2)(q_2^2 - m_{q_2}^2)(p_1^2 - m_{J/\psi}^2)},
 \end{aligned}$$

$$\begin{aligned}
 \mathcal{M}_{\Lambda_c \bar{D}^*} &= \int \frac{d^4q_1}{(2\pi)^4} ig_x^2 \frac{eM_{J/\psi}^2}{f_{J/\psi}} \bar{u}_p(p_4, m_4) (\not{q}_1 + m_{q_1}) u_p(p_2, m_2) \\
 & \times (-g^{\mu\nu} + \frac{q_2^\mu q_2^\nu}{m_{D^*}^2}) \varepsilon_{J/\psi\mu}^*(p_3, m_3) \varepsilon_\gamma^\alpha(p_1, m_1) \\
 & \times \frac{g_{\nu\alpha} \mathcal{F}^2(q_1^2, \Lambda^2)}{(q_1^2 - m_{q_1}^2)(q_2^2 - m_{q_2}^2)(p_1^2 - m_{J/\psi}^2)}.
 \end{aligned}$$

Analysis on $\gamma p \rightarrow J/\psi p$



$$\mathcal{L} = g\bar{U}_N\gamma_5\gamma_\rho(-g^{\rho\mu} + \frac{p^\rho p^\mu}{m^2})U_{P_c}\varepsilon_{J/\psi\mu}^*$$

$$\mathcal{L} = g\bar{U}_N U_{P_c}^\mu \varepsilon_{J/\psi\mu}^*$$

$$\mathcal{M}^{P_c(4312)} = -\frac{eM_{J/\psi}^2}{f_{J/\psi}}\bar{u}_p(p_4, m_4)\gamma_5\tilde{\gamma}_\mu[(\not{p}_1 + \not{p}_2) + m_{P_c(4312)}]$$

$$\times \tilde{\gamma}_\nu\gamma_5 u_p(p_2, m_2)\varepsilon_{J/\psi}^{*\mu}(-g_{\nu\alpha} + \frac{p_{1\nu}p_{1\alpha}}{m_{J/\psi}^2})\varepsilon_{\gamma\alpha}$$

$$\times \frac{g_{P_c(4312)}^2}{((p_1 + p_2)^2 - m_{P_c(4312)}^2)(p_1^2 - m_{J/\psi}^2)},$$

$$\mathcal{M}^{P_c(4380)} = -\frac{eM_{J/\psi}^2}{f_{J/\psi}}\bar{u}_p(p_4, m_4)[(\not{p}_1 + \not{p}_2) + m_{P_c(4380)}]$$

$$\times [-g_{\mu\nu} + \frac{1}{3}\gamma_\mu\gamma_\nu + \frac{1}{3}\frac{\not{q}}{q^2}(\gamma_\mu q_\nu - \gamma_\nu q_\mu) + \frac{2}{3}\frac{q_\mu q_\nu}{q^2}]$$

$$\times u_p(p_2, m_2)\varepsilon_{J/\psi}^{*\mu}(-g^{\nu\alpha} + \frac{p_1^\nu u p_{1\alpha}}{m_1^2})\varepsilon_{\gamma\alpha}$$

$$\times \frac{g_{P_c(4380)}^2}{((p_1 + p_2)^2 - m_{P_c(4380)}^2)(p_1^2 - m_{J/\psi}^2)},$$

$$\mathcal{M}^{P_c(4440)} = -\frac{eM_{J/\psi}^2}{f_{J/\psi}}\bar{u}_p(p_4, m_4)\gamma_5\tilde{\gamma}_\mu[(\not{p}_1 + \not{p}_2) + m_{P_c(4440)}]$$

$$\times \tilde{\gamma}_\nu\gamma_5 u_p(p_2, m_2)\varepsilon_{J/\psi}^{*\mu}(-g_{\nu\alpha} + \frac{p_{1\nu}p_{1\alpha}}{m_{J/\psi}^2})\varepsilon_{\gamma\alpha}$$

$$\times \frac{g_{P_c(4440)}^2}{((p_1 + p_2)^2 - m_{P_c(4440)}^2)(p_1^2 - m_{J/\psi}^2)},$$

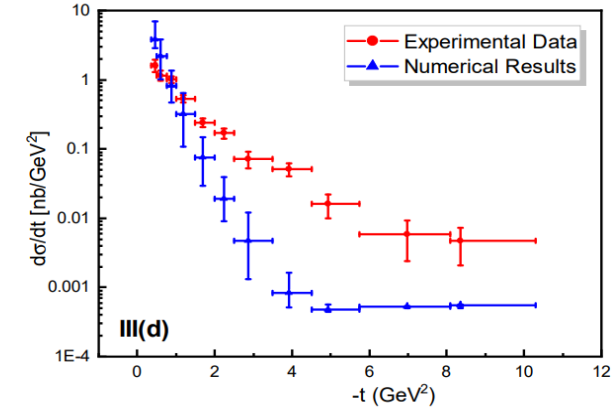
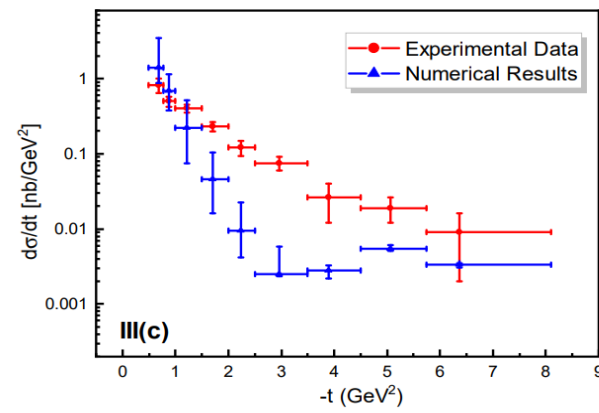
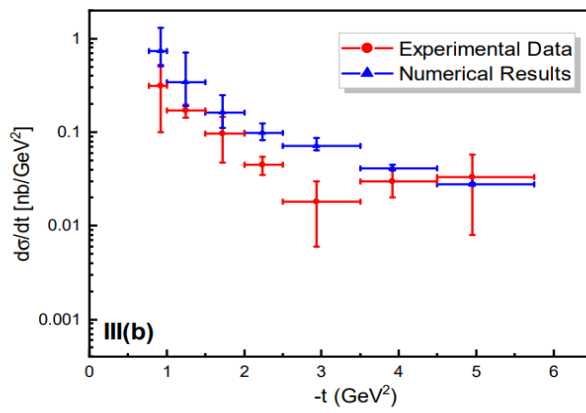
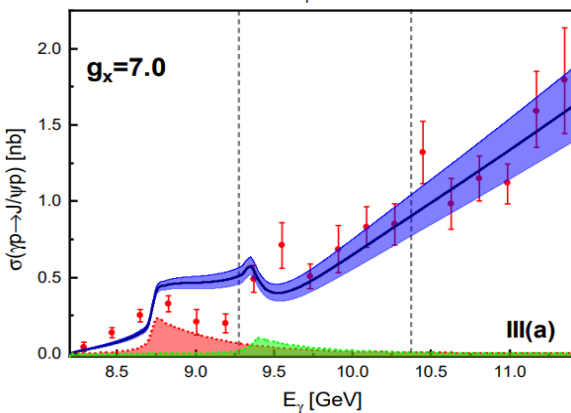
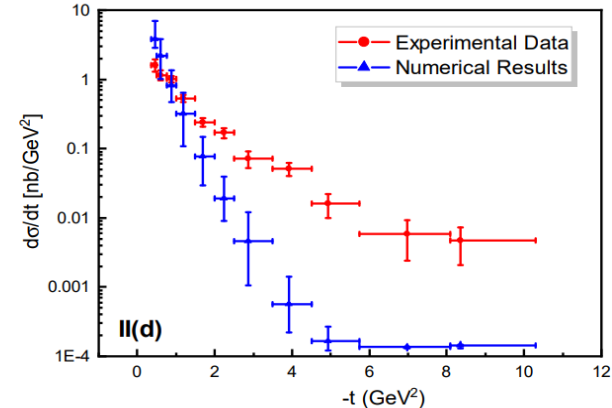
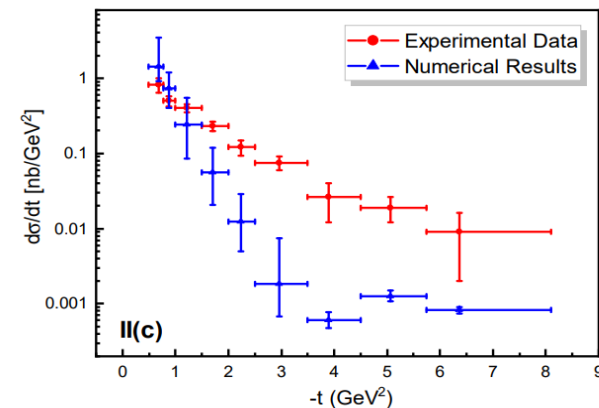
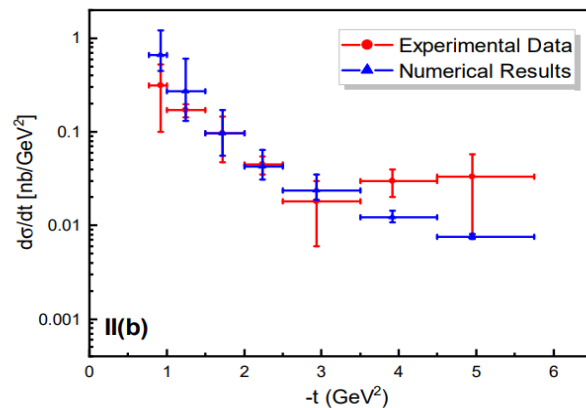
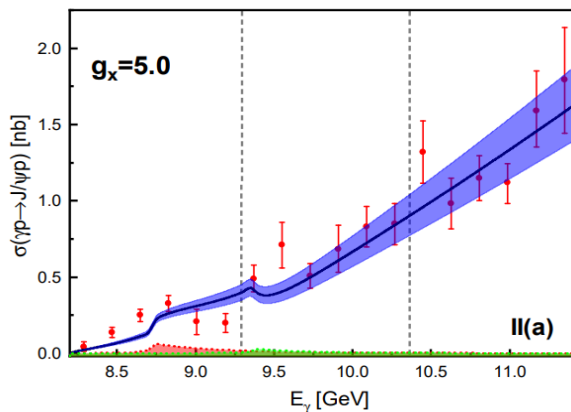
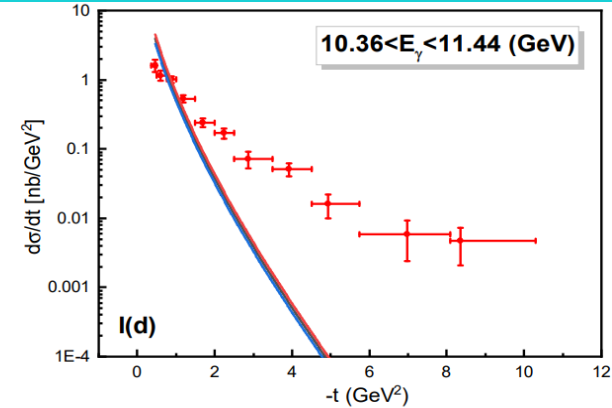
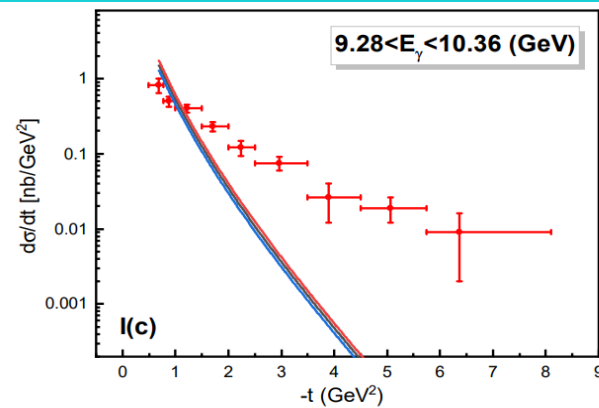
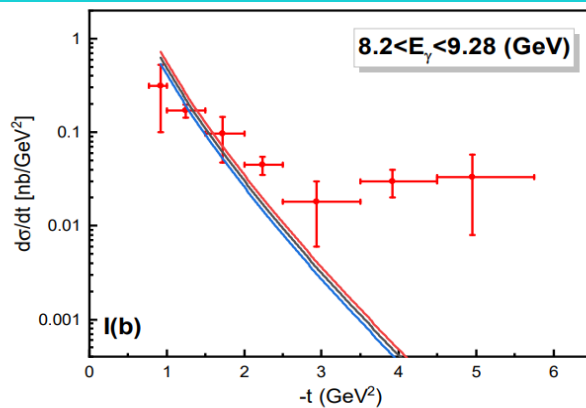
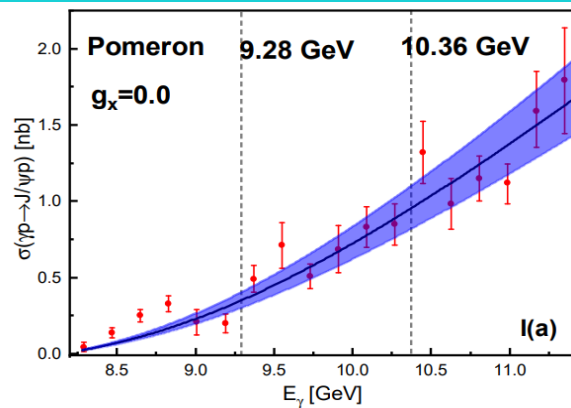
$$\mathcal{M}^{P_c(4457)} = -\frac{eM_{J/\psi}^2}{f_{J/\psi}}\bar{u}_p(p_4, m_4)[(\not{p}_1 + \not{p}_2) + m_{P_c(4457)}]$$

$$\times [-g_{\mu\nu} + \frac{1}{3}\gamma_\mu\gamma_\nu + \frac{1}{3}\frac{\not{q}}{q^2}(\gamma_\mu q_\nu - \gamma_\nu q_\mu) + \frac{2}{3}\frac{q_\mu q_\nu}{q^2}]$$

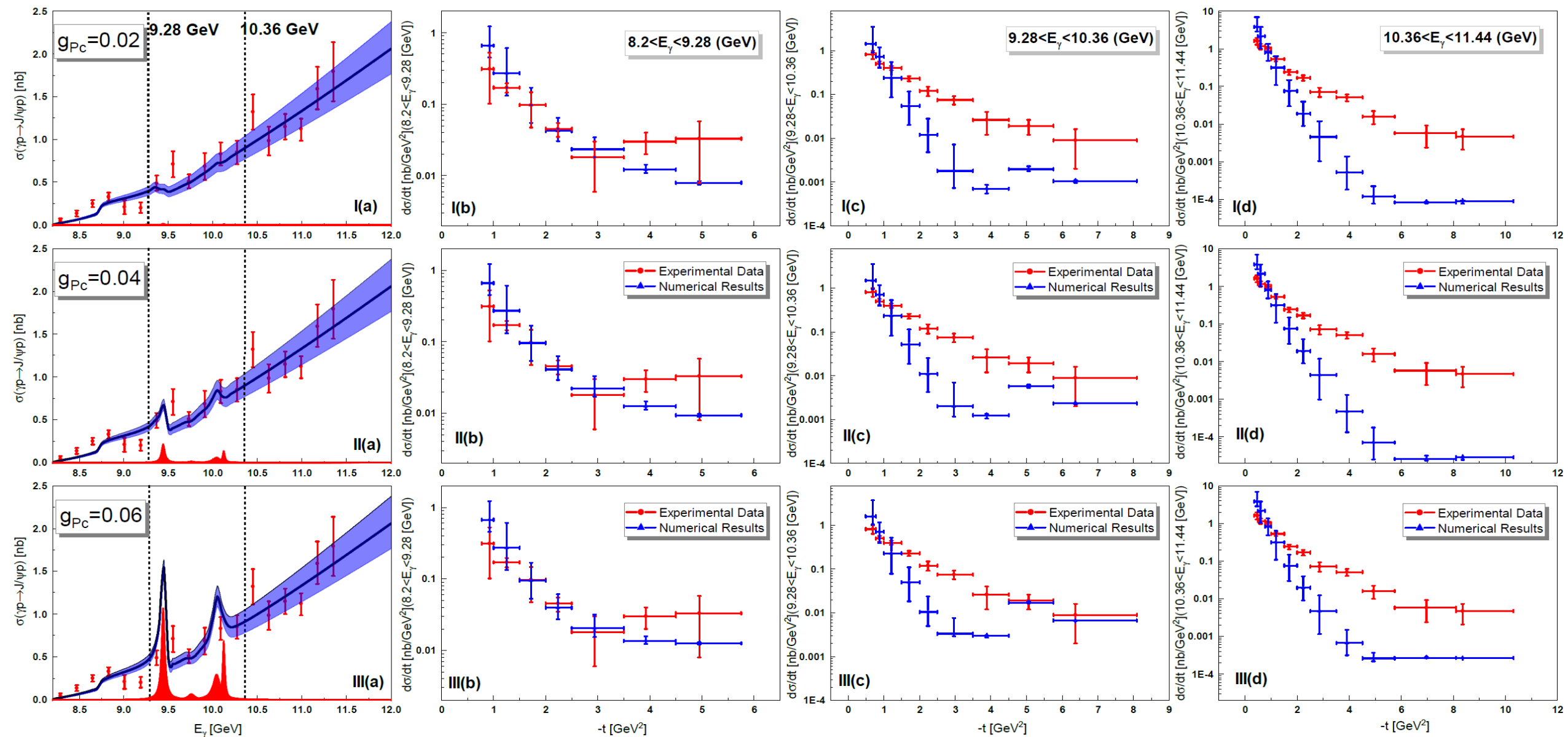
$$\times u_p(p_2, m_2)\varepsilon_{J/\psi}^{*\mu}(-g^{\nu\alpha} + \frac{p_1^\nu u p_{1\alpha}}{m_1^2})\varepsilon_{\gamma\alpha}$$

$$\times \frac{g_{P_c(4457)}^2}{((p_1 + p_2)^2 - m_{P_c(4457)}^2)(p_1^2 - m_{J/\psi}^2)},$$

Numerical results



Numerical results



Numerical results

Coupling
Constants

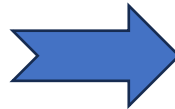


Decay
Widths

TABLE I:

g_{P_c}	0.01	0.02	0.04	0.06
$\Gamma[P_c(4312) \rightarrow J/\psi p]$ (keV)	7.71	30.8	123	277
$\Gamma[P_c(4380) \rightarrow J/\psi p]$ (keV)	2.93	11.7	46.9	105
$\Gamma[P_c(4440) \rightarrow J/\psi p]$ (keV)	9.69	38.8	155	349
$\Gamma[P_c(4457) \rightarrow J/\psi p]$ (keV)	3.31	13.3	53.0	119

Decay width in the
molecular scheme:



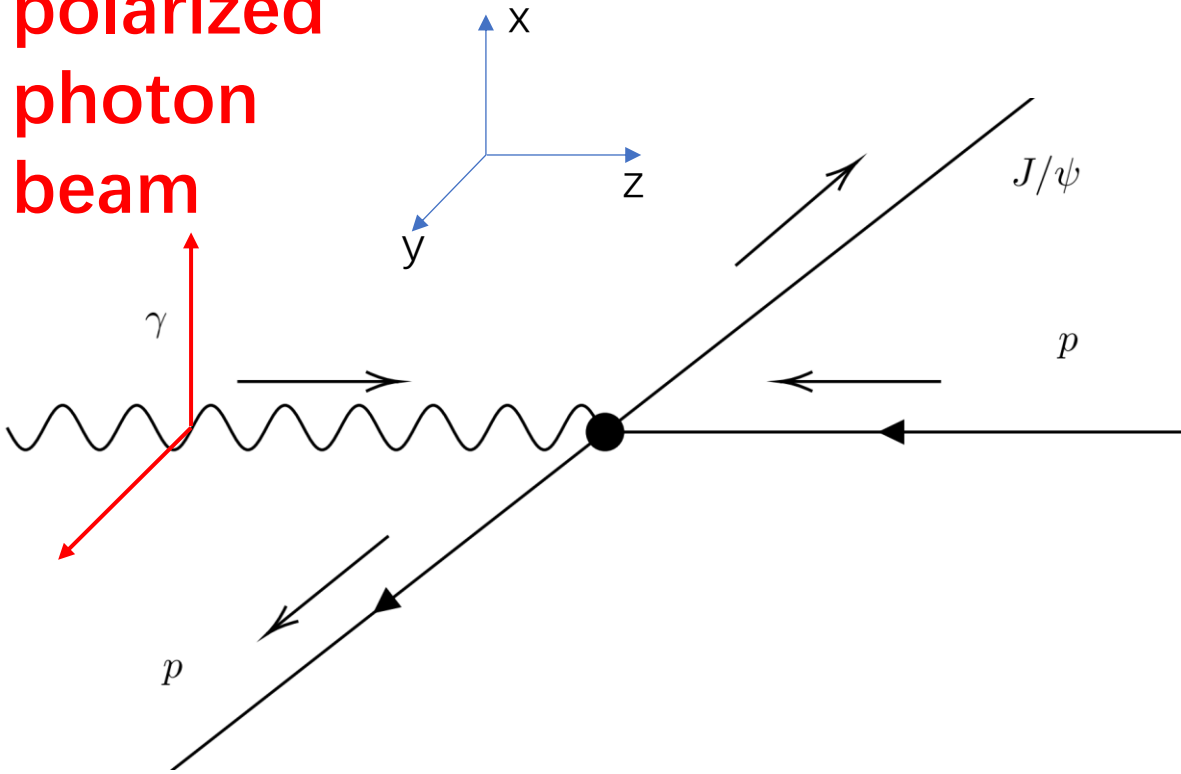
Yong-Hui Lin and Bing-Song Zou
arXiv:1908.05309v1

The coupling constants of $P_c \rightarrow J/\psi p$ determined from $\gamma p \rightarrow J/\psi p$ process are in accordance with the results from the molecular scheme

Mode	Widths (MeV) with (f_1, f_3)					Mode	Widths (MeV) with (f_1, f_3)			
	$\bar{D}\Sigma_c$		$\bar{D}^*\Sigma_c$				$\bar{D}\Sigma_c^*$		$\bar{D}^*\Sigma_c^*$	
	$P_c(4312)$	$P_c(4440)$	$P_c(4457)$		$P_c(4376)$		$P_c(4500)$	$P_c(4511)$	$P_c(4523)$	
	$\frac{1}{2}^-$	$\frac{1}{2}^-$	$\frac{3}{2}^-$	$\frac{1}{2}^-$	$\frac{3}{2}^-$		$\frac{3}{2}^-$	$\frac{1}{2}^-$	$\frac{3}{2}^-$	$\frac{5}{2}^-$
$\bar{D}^*\Lambda_c$	3.8	13.9	6.2	12.5	6.1	$\bar{D}^*\Lambda_c$	12.4	7.1	17.0	4.5
$J/\psi p$	0.001	0.03	0.02	0.02	0.01	$J/\psi p$	0.01	0.006	0.02	0.006
$\bar{D}\Lambda_c$	0.06	5.6	1.7	3.8	1.5	$\bar{D}\Lambda_c$	9^{-5}	10.0	0.3	1.5
πN	0.004	0.002	2^{-4}	0.001	1^{-4}	πN	2^{-4}	0.003	1^{-4}	3^{-4}
$\chi_{c0} p$	-	8^{-4}	4^{-5}	9^{-4}	3^{-5}	$\chi_{c0} p$	0.003	0.01	0.002	6^{-7}
$\eta_c p$	0.01	3^{-4}	8^{-5}	2^{-4}	6^{-5}	$\eta_c p$	0.001	0.01	6^{-4}	8^{-4}
ρN	3^{-5}	3^{-4}	4^{-5}	2^{-4}	2^{-5}	ρN	5^{-4}	0.001	0.01	8^{-5}
ωp	1^{-4}	0.001	2^{-4}	6^{-4}	9^{-5}	ωp	0.002	0.004	0.005	3^{-4}
$\bar{D}\Sigma_c$	-	3.4	0.5	2.6	1.0	$\bar{D}\Sigma_c$	5^{-4}	10.6	0.2	1.3
$\bar{D}\Sigma_c^*$	-	0.8	5.4	1.9	6.2	$\bar{D}\Sigma_c^*$	-	1.0	33.8	6.2
Total	3.9	23.7	13.9	20.7	14.7	$\bar{D}^*\Sigma_c$	-	10.6	0.07	1.2
						$\bar{D}\Lambda_c\pi$	5.0	-	-	-
						$\bar{D}^*\Lambda_c\pi$	-	4.0	7.7	7.8
						Total	17.5	43.3	59.1	22.5

Beam Asymmetry

polarized
photon
beam



$$\begin{aligned} \check{\Sigma} &= \frac{1}{2} \{ -H_{1-1}^r H_{41}^r - H_{1-1}^i H_{41}^i + H_{10}^r H_{40}^r + H_{10}^i H_{40}^i \\ &\quad - H_{11}^r H_{4-1}^r - H_{11}^i H_{4-1}^i + H_{2-1}^r H_{31}^r + H_{2-1}^i H_{31}^i \\ &\quad - H_{20}^r H_{30}^r - H_{20}^i H_{30}^i + H_{21}^r H_{3-1}^r + H_{21}^i H_{3-1}^i \} \\ &= \frac{1}{2} \langle H | \Gamma^4 \omega^A | H \rangle. \end{aligned}$$

$$\varepsilon_\gamma^{+1} = \frac{-1}{\sqrt{2}}(0, 1, i, 0), \quad \varepsilon_\gamma^{-1} = \frac{1}{\sqrt{2}}(0, 1, -i, 0),$$

$$\varepsilon_\gamma^x = -\frac{1}{\sqrt{2}}(\varepsilon_\gamma^{+1} - \varepsilon_\gamma^{-1}) = (0, 1, 0, 0),$$

$$\varepsilon_\gamma^y = \frac{i}{\sqrt{2}}(\varepsilon_\gamma^{+1} + \varepsilon_\gamma^{-1}) = (0, 0, 1, 0).$$

$$\mathcal{M}^{\lambda_\gamma \lambda_i \lambda_f \lambda_V} = \langle \varepsilon_{J/\psi}^{\lambda_V}(p_3, m_3) \bar{u}_p^{\lambda_f}(p_4, m_4) | \hat{T} | u_p^{\lambda_i}(p_2, m_2) \varepsilon_\gamma^{\lambda_\gamma}(p_1) \rangle,$$

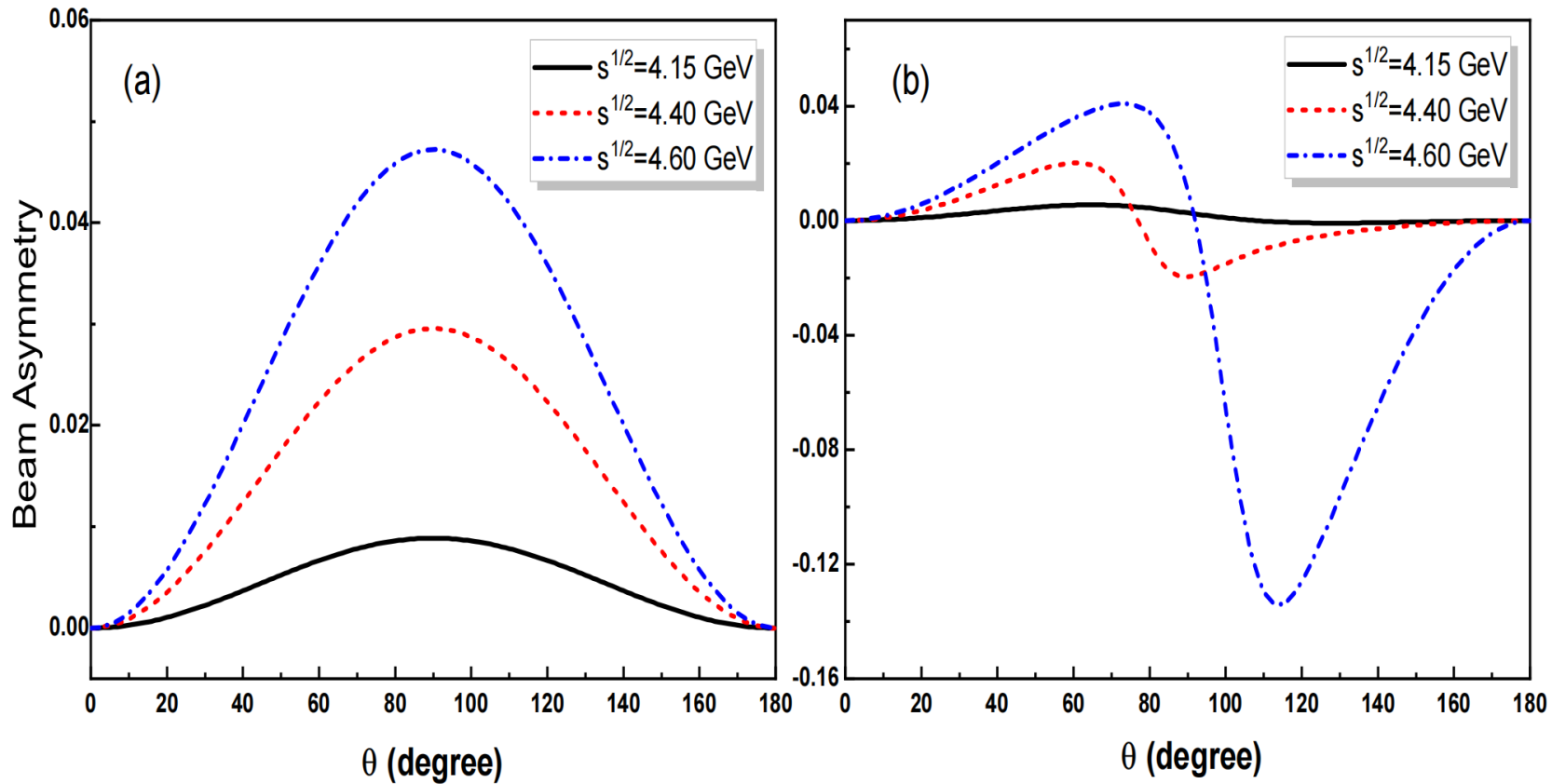
$$\mathcal{M}_x = \sum_{\lambda_{i,f}=\pm\frac{1}{2}} \sum_{\lambda_V=\pm 1,0} \frac{-1}{\sqrt{2}} (\mathcal{M}_{\lambda_\gamma=+1}^{\lambda_i \lambda_f \lambda_V} - \mathcal{M}_{\lambda_\gamma=-1}^{\lambda_i \lambda_f \lambda_V})$$

$$\mathcal{M}_y = \sum_{\lambda_{i,f}=\pm\frac{1}{2}} \sum_{\lambda_V=\pm 1,0} \frac{i}{\sqrt{2}} (\mathcal{M}_{\lambda_\gamma=+1}^{\lambda_i \lambda_f \lambda_V} + \mathcal{M}_{\lambda_\gamma=-1}^{\lambda_i \lambda_f \lambda_V})$$

$$\check{\Sigma} = \frac{d\sigma_x - d\sigma_y}{d\sigma_x + d\sigma_y}$$

- [1] PRC 71,054004
[2] Rep. Prog. Phys. 57,1

Beam Asymmetry



Only t-channel (Pomeron)

t-channel + s-channel
(Pomeron + Pc + Cusps)

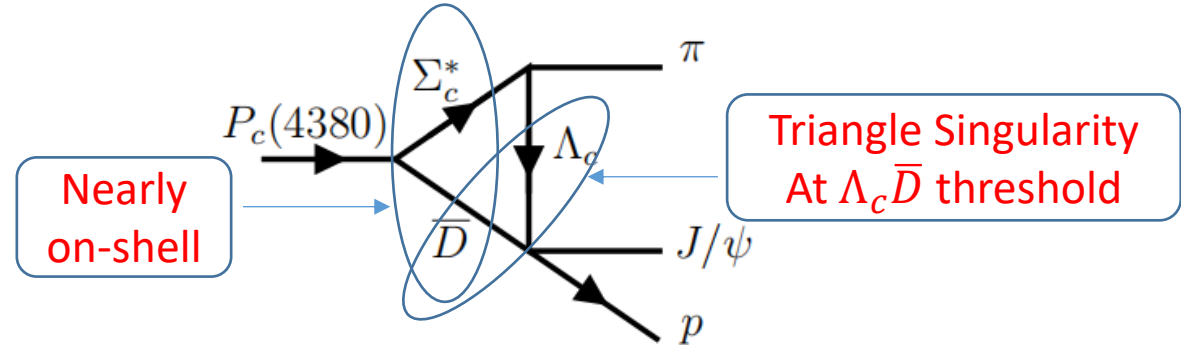
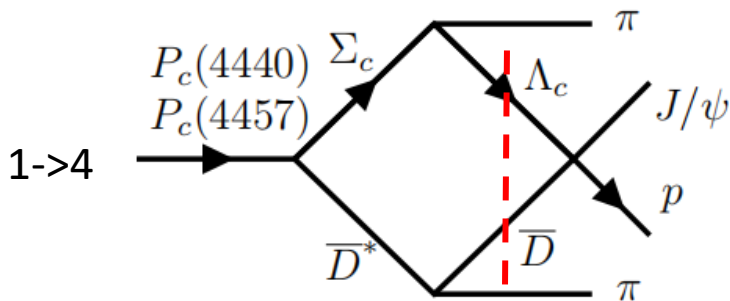
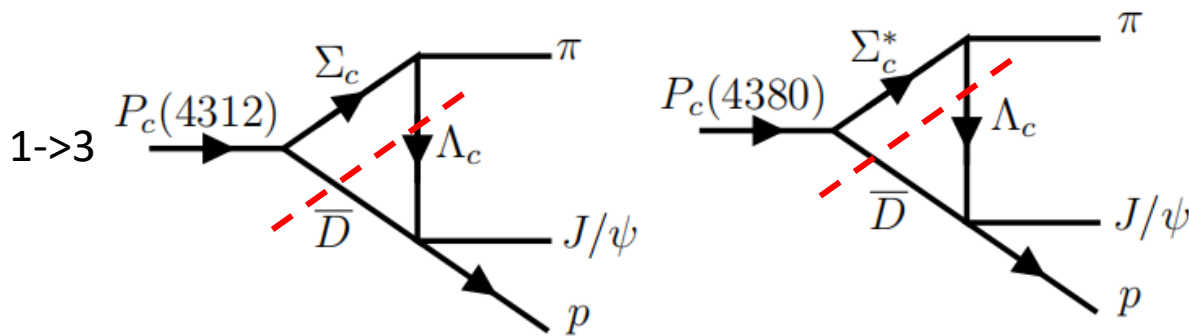
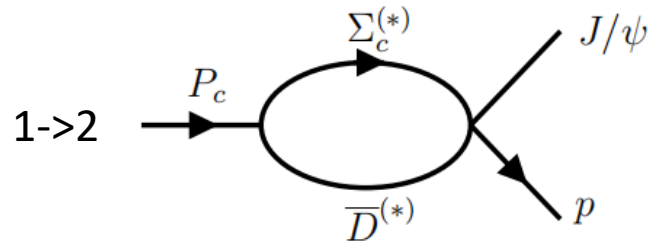
1). The Beam Asymmetry is not big in $\gamma p \rightarrow J/\psi p$ scattering.

2). The Beam Asymmetry in t-channel is very different from that in s-channel plus t-channel. (node)

3). The Beam Asymmetry explicitly indicates the existence of the s-channel contribution.

Feed-down phenomenon of P_c states

Besides the 2-body decay of P_c states, the 3-body and 4-body decay processes show **some unique phenomena from molecular P_c states and Triangle/Box Singularity**.



1. A molecular P_c can only couple to $\Sigma_c^{(*)} \bar{D}^{(*)}$ which is the component of the P_c
2. $\Sigma_c^* \rightarrow \Lambda_c \pi$ and $D^* \rightarrow D \pi$ processes induce a π emission process in P_c decay.

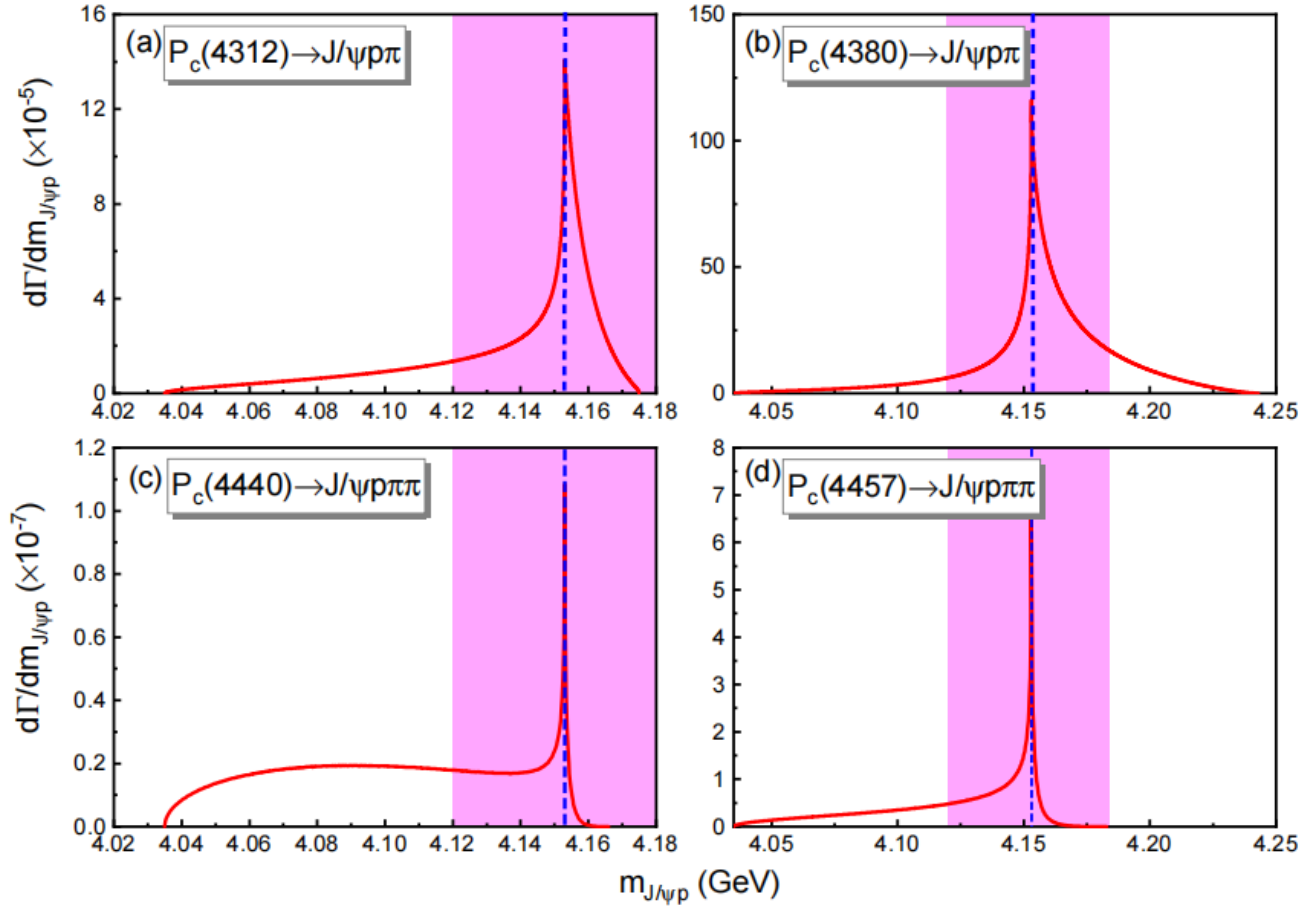


$\Lambda_c \bar{D}$ cut appears in the $J/\psi p$ invariant mass spectrum of $P_c \rightarrow J/\psi p \pi(\pi)$

Feed-down peak: a TS(BS) peak around $\Lambda_c \bar{D}$ threshold can be observed in the $J/\psi p$ invariant mass spectrum.

Feed-down phenomenon of P_c states

$J/\psi p$ invariant mass spectrum in $P_c \rightarrow J/\psi p \pi(\pi)$:



I. The enhancement peak around $\Lambda_c \bar{D}$ threshold on $J/\psi p$ spectrum from our calculation was shown.

II. Comparing to the results from TS diagram, the contribution from BS mechanism induces a narrow peak with smaller value.

III. With a comparison, the $P_c(4380)$ is proved to be the important initial state, since the contribution from $P_c(4380)$ is much larger than others.

PHYSICAL REVIEW D **109**, L031507 (2024)

Letter

Predictions for feed-down enhancements at the $\Lambda_c \bar{D}$ and $\Lambda_c \bar{D}^*$ thresholds via the triangle and box singularities

Ming-Xiao Duan^{1,*}, Lin Qiu^{1,2}, Xi-Zhe Ling¹ and Qiang Zhao^{1,2,†}

¹Institute of High Energy Physics, Chinese Academy of Sciences, Beijing 100049, People's Republic of China

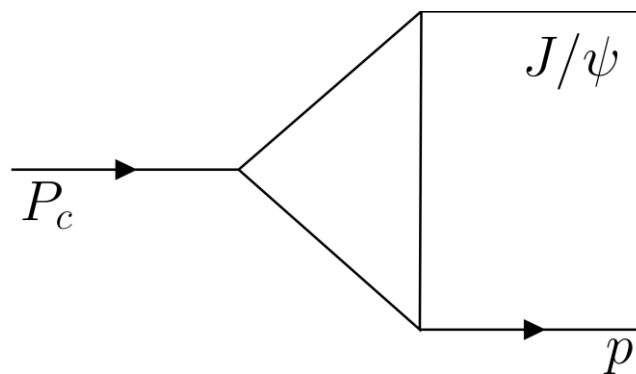
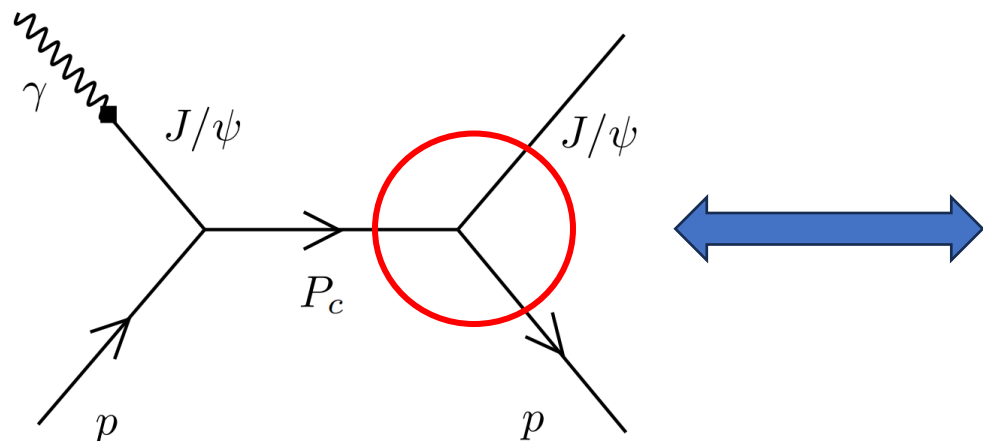
²University of Chinese Academy of Sciences, Beijing 100049, People's Republic of China

Summary

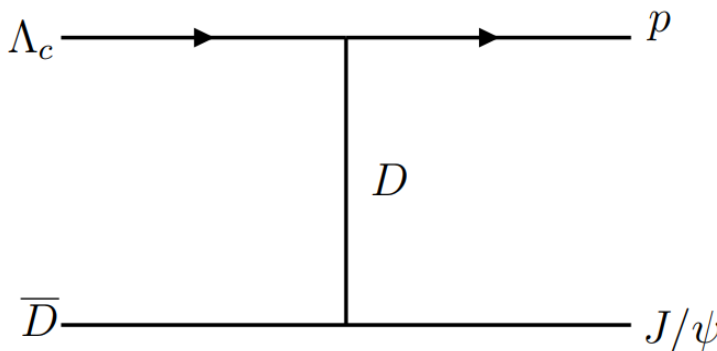
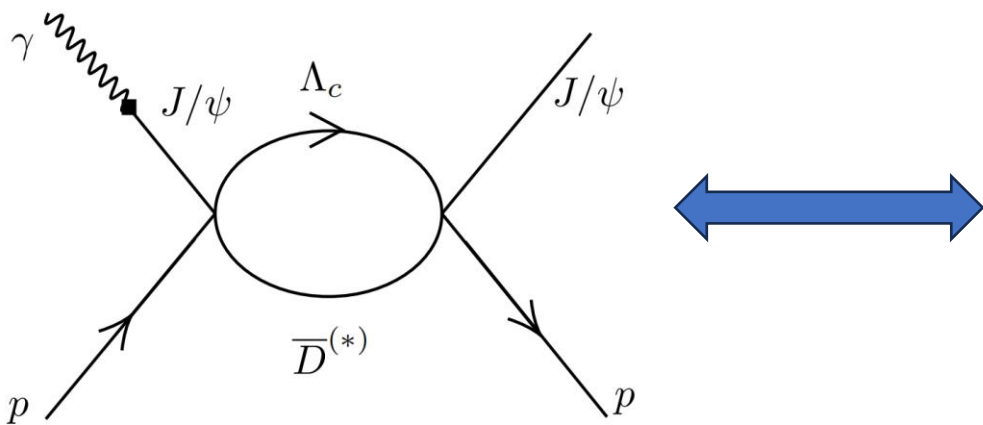
- 1). We have studied the $\gamma p \rightarrow J/\psi p$ process in the t channel and s channel with Pomeron, P_c , and $\Lambda_c \bar{D}$ bubble.
- 2). The Pomeron exchange is found to be the dominate part in the $\gamma p \rightarrow J/\psi p$ process.
- 3). The s channel contributions also can not be ignored in the analysis.
- 4). The Beam Asymmetry is given to show the existence of the s channel contribution in the photoproduction.
- 5). The feed down phenomenon from the 3/4-body decay of P_c is also introduced.

Thank you

Numerical results



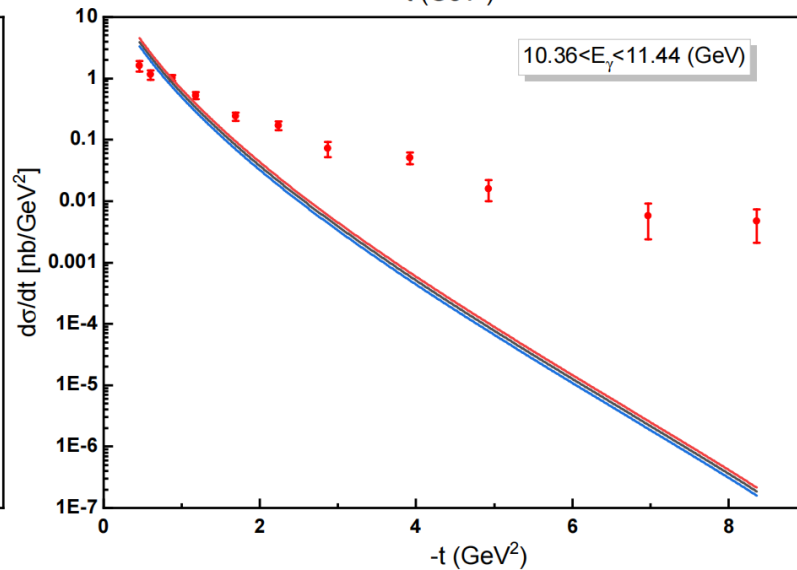
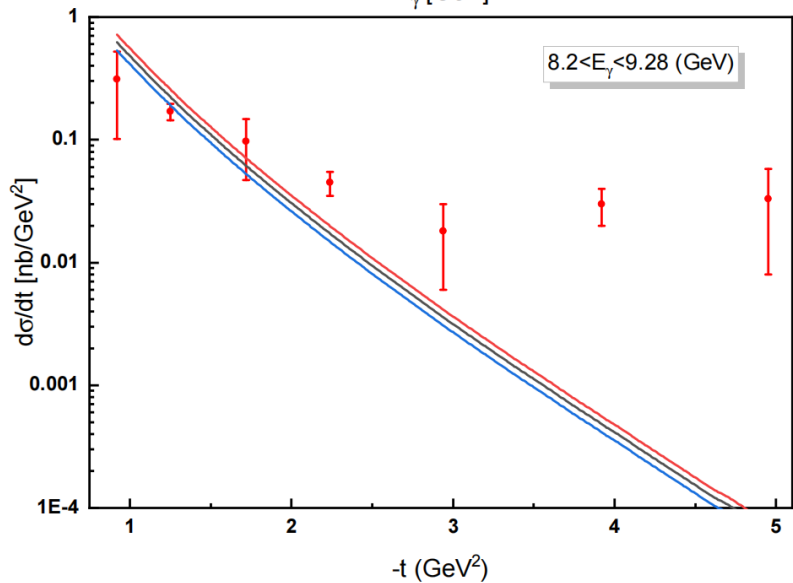
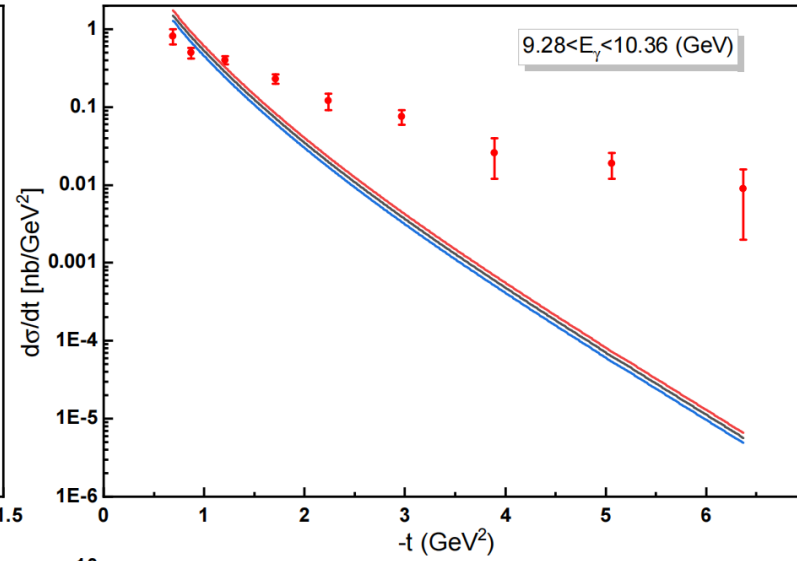
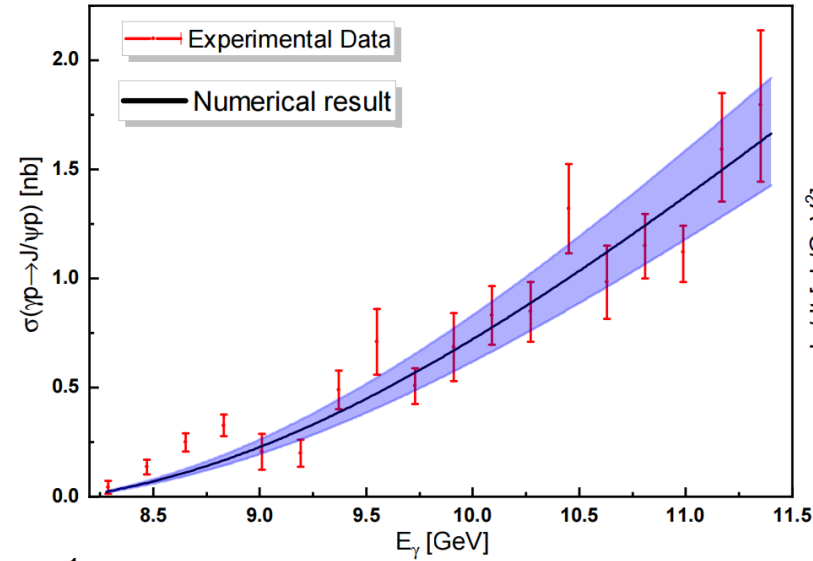
Double suppressed
by both the
production and
decay process



$g_{\Lambda_c \bar{D} J/\psi p} = 3.0$ Estimated from
 $g_{\Lambda_c \bar{D}^* J/\psi p} = 8.4$ t-channel

$g_{\Lambda_c \bar{D} J/\psi p} = g_{\Lambda_c \bar{D} J/\psi p} = 6.0$ is
employed in the calculation

Analysis on $\gamma p \rightarrow J/\psi p$



Pomeron contribution

$\beta_c = 0.25, 0.27, 0.29 \text{ GeV}^{-1}$,
The total and differential cross section of the process can be obtained.

1). The numerical cross section can explain the experimental data generally.

2). The differential cross section can not be explained by the pomeron exchange process.

Analysis on $\gamma p \rightarrow J/\psi p$

Experimental aspect

- 1). The experimental results are determined from the distribution of t and E .
- 2). In the calculation, we should also include the distribution of t and E .
- 3). Through a calculation, we find the distribution of E will not obviously influence the differential cross section.

TABLE IV. $\gamma p \rightarrow J/\psi p$ differential cross sections in the 8.2 – 9.28 GeV beam energy range, average t and beam energy in bins of t . The first cross section uncertainties are statistical, and the second are systematic. The overall average beam energy is 8.93 GeV.

t bin [GeV ²]	$\langle t \rangle$ [GeV ²]	$\langle E_\gamma \rangle$ [GeV]	$d\sigma/dt$ [nb/GeV ²]
0.77 – 1.00	0.92	9.14	$0.313 \pm 0.092 \pm 0.120$
1.00 – 1.50	1.25	8.96	$0.170 \pm 0.018 \pm 0.008$
1.50 – 2.00	1.72	8.80	$0.097 \pm 0.010 \pm 0.040$
2.00 – 2.50	2.24	8.77	$0.045 \pm 0.007 \pm 0.003$
2.50 – 3.50	2.94	8.78	$0.018 \pm 0.003 \pm 0.009$
3.50 – 4.50	3.92	8.95	$0.030 \pm 0.006 \pm 0.004$
4.50 – 5.75	4.95	9.10	$0.033 \pm 0.013 \pm 0.012$

